Electrical properties of $m \times n$ cylindrical network*

Zhi-Zhong Tan(谭志中)[1,†] and Zhen Tan(谭震)[2]

[1] *Department of Physics, Nantong University, Nantong* 226019, *China*
[2] *School of Information Science and Technology, Nantong University, Nantong* 226019, *China*

(Received 26 February 2020; revised manuscript received 18 May 2020; accepted manuscript online 27 May 2020)

We consider the problem of electrical properties of an $m \times n$ cylindrical network with two arbitrary boundaries, which contains multiple topological network models such as the regular cylindrical network, cobweb network, globe network, and so on. We deduce three new and concise analytical formulae of potential and equivalent resistance for the complex network of cylinders by using the RT-V method (a recursion-transform method based on node potentials). To illustrate the multiplicity of the results we give a series of special cases. Interestingly, the results obtained from the resistance formulas of cobweb network and globe network obtained are different from the results of previous studies, which indicates that our research work creates new research ideas and techniques. As a byproduct of the study, a new mathematical identity is discovered in the comparative study.

Keywords: cylindrical network, complex boundaries, RT-V method, electrical properties, Laplace equation

PACS: 05.50.+q, 84.30.Bv, 89.20.Ff, 02.10.Yn **DOI:** 10.1088/1674-1056/ab96a7

1. Introduction

Resistor network research involves a wide range of fields, not only of electrical problems but also of non-electric problems, such as chaotic quantum billiards that are simulated by a circuit network,[1] waveguides in photonic crystals,[2] a simulation of a non-Abelian Aharonov–Bohm effect,[3] the electrical properties of conducting meshes,[4] field theory for scale-free random networks,[5] lattice Green's functions,[6–8] finite difference time-domain method for electromagnetic waves,[9] *etc*. In particular, researchers can study the Laplace equation and Poisson equation[10] by the resistor network model. In addition, the resistor network model has been published in journals of various disciplines, including chemical, physical chemistry, discrete mathematics, applied mathematics, engineering technology, physics, and so on. Specifically, the muhigrid method for three-dimensional (3D) modeling of Poisson equation published in Ref. [11]; resistance distance published in Refs. [12,13]; resistance distance and Laplacian spectrum published in Ref. [14]; a recursion formula for resistance distances and its applications and resistance distance in complete n-partite graphs published in Refs. [15,16]; resistances between two nodes of a path network published in Ref. [17]; resistance distances in corona and neighborhood corona networks based on Laplacian generalized inverse approach published in Ref. [18]; resistance distances in composite graphs and some rules on resistance distance with applications published in Refs. [19,20]; resistance between two nodes of a ring network published in Ref. [21]; universal relation for transport in non-sparse complex networks published in Ref. [22]; two-point resistance on the centered-triangular lattice published in Ref. [23]; exact evaluation of the resistance in an infinite face-centered cubic network published in Ref. [24]; resistance calculation of infinite three-dimensional triangular and hexagonal prism lattices published in Ref. [25], and so on. The above researches show that the research of resistor network model has important theoretical value and potential application value in many fields.

As is well known, computing the effective resistance between any two nodes in a resistor network is a difficult problem because it is required to solve the complex circuits and complex matrix equations. For example, it may be difficult to obtain the explicit expression of potential and resistance of the complex networks with arbitrary boundaries when the boundary resistor is complex. In fact, the boundary conditions are very binding and will affect the calculation method and process of the problem. Therefore, the solution of each complex resistor network problem needs to create innovative ideas and methods.

The resistor network research has been done for a long time. In 1845 Kirchhoff established the basic circuit theory. 150 years later, Cserti[6] studied the infinite resistor network by Green's function technique, which is not suitable for computing finite lattices. After some applications,[23–25] some new issues were investigated by the Green's function technique. In order to solve the problem of finite resistor network, in 2004 Wu[26] presented a Laplacian matrix method, the method is suitable for the lattice in definite and canonical boundary conditions. The main weakness of this method is that it needs to find the eigenvalues and eigenvectors of the matrices with two directions, which makes it impossible to solve the resistor

*Project supported by the Natural Science Foundation of Jiangsu Province, China (Grant No. BK20161278).
†Corresponding author. E-mail: tanz@ntu.edu.cn

network with arbitrary boundaries. After 2004, several new problems of resistor network were studied by the Laplacian matrix approach.[27–32] From the above analysis, the Green function method and the Laplace method cannot solve the resistor network problem with arbitrary boundaries, but the resistor networks with arbitrary boundaries come from reality, and they need to be solved by researchers. Fortunately, in 2011 Tan created a new theory for studying arbitrary resistor networks,[33] which now is called recursion–transform (RT) theory of Tan.[29] The advantage of the RT method is that it depends on a matrix in only one direction and the result is expressed by a single sum. With the development of the RT technique, a series of new resistor networks with zero resistor edges was solved.[34–44] Recently, the Recursion–Transform method was subdivided into two ways: one way is to use current parameters to set up matrix equations,[36–42] which is simply called the RT-I method; another way is to use potential parameters to set up matrix equations,[43,44] which is simply called the RT-V method.

Investigations showed that many previous applications of the RT (including RT-I and RT-V) theory focus on resistor networks with zero resistor boundaries or special cases, such as the globe network[34,42] belongs to cylindrical network with two zero resistor boundaries, the cobweb network[32,36,43] belongs to cylindrical network with one zero resistor boundary, *et al.* Obviously, the complex resistor network without zero resistance boundary condition also needs to be studied. Very recently, new progress has been made: in Ref. [45] the n-step network with Δ structure was studied, in Ref. [46] the electrical characteristics of rectangular network was investigated by using the RT-V method, In Ref. [47] the electrical characteristics of arbitrary rectangular network with an arbitrary right boundary was studied by the RT-I approach. In Ref. [48] a new resistor network theory was developed by unifying the rectangular network and cylindrical network. However, because of the multifunctional nature of a cylindrical network with two arbitrary boundaries, the authors in Ref. [48] have not completely studied the conventional $m\times n$ cylindrical network (it sees cylindrical networks as just one example of the basic theory), and it is difficult for readers understand the results it gives. Therefore, in this paper we will systematically introduce the complete research process of cylindrical network, and take $\square\times n$ and $\Delta\times n$ for example to help readers understand the physical implications of the results.

Consider a complex and anisotropic $m\times n$ cylindrical resistor network as shown in Fig. 1, in which the grid layout is continuous and the resistors are distributed anisotropy. In this figure n and m denote the numbers of resistors along the horizontal and cycle directions respectively, and the resistors r and r_0 in the respective horizontal (longitude) and loop (cycle or latitude) directions except for two arbitrary boundary resistors of r_1 and r_2. The difference between r and r_0 in horizontal and cycle directions implies the anisotropy of the network. This paper focused on studying the electrical characteristics (resistance and potential) of a cylindrical $m\times n$ resistor network with two arbitrary boundaries by using the advanced RT-V method, and we build three new theoretical formulae, thus lead large problems to be resolved. Studies have shown that the complex cylindrical networks with arbitrary boundaries are the multifunctional network model because it can deduce various geometrical structures (Figs. 3–6 and 12). Thus a large number of problems of resistor networks will be resolved in this paper. We emphasize that what was studied in Ref. [40] is only a special cylindrical network (with a zero resistance on the bottom), but our research on a cylindrical network is a general case of the network, which is completely different from the scenario in Ref. [40] and to our knowledge, it has not been studied before.

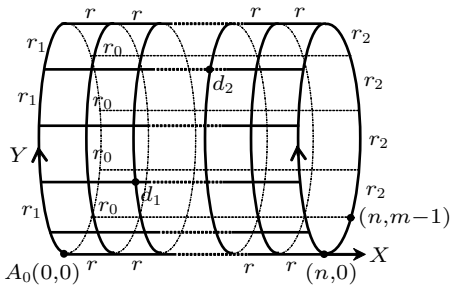

Fig. 1. Nonregular cylindrical $m\times n$ resistor network, where m and n are the numbers of resistors along the cycle and horizontal directions respectively, with unit resistors r and r_0 in the respective horizontal and loop directions except for two arbitrary boundary resistors of r_1 and r_2.

For the sake of comparative study, here we introduce a main result of cylindrical network. In 2004 Wu[26] gave the accurate equivalent resistance of the regular cylindrical network by the Laplacian matrix approach for the first time. The so-called regular network refers to the boundary resistors $r_1=r_2=r_0$ in Fig. 1.

Consider a normative $m\times n$ cylindrical resistor network ($r_1=r_2=r_0$), where n and m are the numbers of resistors along the horizontal and cycle directions respectively, and r and r_0 are, respectively, the resistors along the horizontal and loop directions, Wu[26] gave the resistance between two nodes $d_1(x_1,y_1)$ and $d_2(x_2,y_2)$ as follows:

$$\begin{aligned} &R_{m\times n}(d_1,d_2)\\ &=\frac{r_0}{n+1}\left(|y_1-y_2|-\frac{(y_1-y_2)^2}{m}\right)\\ &\quad+\frac{r}{m}|x_1-x_2|+\frac{1}{m(n+1)}\sum_{i=1}^{m-1}\\ &\quad\times\sum_{j=1}^{n}\frac{C_{x_1,j}^2+C_{x_2,j}^2-2C_{x_1,j}C_{x_2,j}\cos(y_2-y_1)\theta_i}{r_0^{-1}(1-\cos\theta_i)+r^{-1}(1-\cos\phi_j)}, \end{aligned}\tag{1}$$

where $C_{x_k,j}=\cos(x_k+1/2)\phi_j$, $\theta_i=2i\pi/m$, $\phi_j=j\pi/(n+1)$.

Formula (1) is found for the first time by Wu. However, when the boundary resistor r_1 and r_2 are the arbitrary

elements, the problem becomes an unresolved difficulty. In addition, the equivalent resistance of Eq. (1) is in the double summations not in a single sum.

The innovation and contribution of this paper is reflected in the four aspects as follows. The first aspect is to generalize the RT theory, for example, previous RT theory relies on the boundary condition of the zero resistance, but it no longer depends on this condition in this paper. The second aspect is the innovation of matrix calculation, for example, the previous matrix transformation is all real numbers, but in this paper, the plural matrix transformation is established (see Eqs. (23) and (44) below). The third aspect is the analytical expressions of the potential function and the equivalent resistance of a complex cylindrical network with two arbitrary boundaries are given for the first time in this paper, and a series of applications are given. The fourth aspect is the discovery of a new mathematical identity from the point of view of physics, which promotes the research and development of mathematical identity.

2. General results of electrical properties

2.1. Several parameter definitions

This article involves a more complex network problem, and the expression of the result is more complex. Some parameters are specifically defined here to simplify the expressions of results

$$C_{y_k-y}^{(i)} = \cos(y_k - y)\theta_i, \theta_i = 2i\pi/m, \tag{2}$$

$$\lambda_i = h + 1 - h\cos\theta_i + \sqrt{(h+1-h\cos\theta_i)^2 - 1},$$

$$\bar{\lambda}_i = h + 1 - h\cos\theta_i - \sqrt{(h+1-h\cos\theta_i)^2 - 1}, \tag{3}$$

with $h = r/r_0$. Defining $h_s = r_s/r_0$ $(s = 1, 2)$, where r_s and r_0 are the resistors in the network of Fig. 1, and defining

$$F_k^{(i)} = (\lambda_i^k - \bar{\lambda}_i^k)/(\lambda_i - \bar{\lambda}_i), \Delta F_k^{(i)} = F_{k+1}^{(i)} - F_k^{(i)}, \tag{4}$$

$$\alpha_{s,x}^{(i)} = \Delta F_x^{(i)} + (h_s - 1)\Delta F_{x-1}^{(i)}, h_s = r_s/r_0, \tag{5}$$

$$\beta_{x\vee x_s}^{(i)} = \begin{cases} \beta_{x,x_s}^{(i)} = \alpha_{1,x}^{(i)}\alpha_{2,n-x_s}^{(i)}, & \text{if } x \leqslant x_s, \\ \beta_{x_s,x}^{(i)} = \alpha_{1,x_s}^{(i)}\alpha_{2,n-x}^{(i)}, & \text{if } x \geqslant x_s, \end{cases} \tag{6}$$

$$G_n^{(i)} = F_{n+1}^{(i)} + (h_1 + h_2 - 2)F_n^{(i)} + (h_1 - 1)(h_2 - 1)F_{n-1}^{(i)}. \tag{7}$$

The above definitions of Eqs. (2)–(7) are used throughout the paper, unless otherwise stated. In order to reduce the repetition of the following expressions, a set of uniform definitions is given here. To help the readers understand the meaning of each symbol, their explanations are given below. Equations (5)–(7) appear in all the equations of this paper because the expression of the electrical characteristics of the network depends on $\alpha_{k,s}^{(i)}$, $\beta_{k,s}^{(i)}$, and $G_k^{(i)}$, and they are composition functions of $F_k^{(i)}$ in Eq. (4), closely related, $F_k^{(i)}$ is a function of λ_i and $\bar{\lambda}_i$, where θ_i in Eq. (3) is determined in Eq. (2).

In a nutshell, the above definitions of Eqs. (2)–(7) are used throughout the paper. When you look at the calculation below you will see that it is necessary to define a series of functions because the electrical properties of the resistor network are more complex, and these definitions are innovative.

2.2. Potential expression of any node

Consider a complex $m \times n$ cylindrical network shown in Fig. 1, two arbitrary resistors are placed on the left- and right-hand side of the network, where the resistor parameters r_i and voltage parameters $V_x^{(y)}$ are shown in Figs. 1 and 2, and the origin of the rectangular coordinate system is specified at point $A_0(0,0)$. Assume that the electric current J goes from the $d_1(x_1, y_1)$ to the $d_2(x_2, y_2)$. Expressing the nodal potential at $d(x,y)$ by $U_{m\times n}(x,y) = V_x^{(y)}$ and choosing the reference potential such that $\sum_{i=0}^{m-1} V_0^{(i)} = 0$, which means hat the sum of the voltages of all the nodes on the left boundary is zero, the analytic expression of the potential function of $d(x,y)$ in the cylindrical $m \times n$ resistor network can be written as

$$\frac{U_{m\times n}(x,y)}{J} = \frac{x_1 - x_\tau}{m} r + \frac{r_0}{2m}\sum_{i=1}^{m-1} \frac{\beta_{x_1\vee x}^{(i)} C_{y_1-y}^{(i)} - \beta_{x_2\vee x}^{(i)} C_{y_2-y}^{(i)}}{(1-\cos\theta_i) G_n^{(i)}}, \tag{8}$$

where $\theta_i = 2i\pi/m$, x_τ is a piecewise function

$$x_\tau = \{x_1, 0 \leqslant x \leqslant x_1\} \cup \{x, x_1 \leqslant x \leqslant x_2\} \cup \{x_2, x_2 \leqslant x \leqslant n\}, \tag{9}$$

and $\beta_{k,s}^{(i)}$ and $G_k^{(i)}$ are defined in Eqs. (6) and (7) respectively.

When taking the reference voltage by $\sum_{i=0}^{m-1} V_n^{(i)} = 0$, which means that the sum of the voltages of all the nodes on the right boundary is zero, the potential function of $d(x,y)$ is

$$\frac{U_{m\times n}(x,y)}{J} = \frac{x_2 - x_\tau}{m} r + \frac{r_0}{2m}\sum_{i=1}^{m-1} \frac{\beta_{x_1\vee x}^{(i)} C_{y_1-y}^{(i)} - \beta_{x_2\vee x}^{(i)} C_{y_2-y}^{(i)}}{(1-\cos\theta_i) G_n^{(i)}}, \tag{10}$$

where all the parameters are the same as the above. Please note that the difference between Eq. (8) and Eq. (10) lies only in the difference in their first term, but the remaining terms are the same, which indicates that the choice of different reference points only affects the first factor of the equation.

Why do we define Eq. (9)? This is because equations (8) and (10) have to be expressed by three piecewise equations if there is no definition of Eq. (9). To understand Eqs. (8) and (9), given here is the explanation: when $0 \leqslant x \leqslant x_1$, there is $x_1 - x_\tau = 0$; when $x_1 \leqslant x \leqslant x_2$, there is $x_1 - x_\tau = x_1 - x$; when $x_2 \leqslant x \leqslant n$, there is $x_1 - x_\tau = x_1 - x_2$.

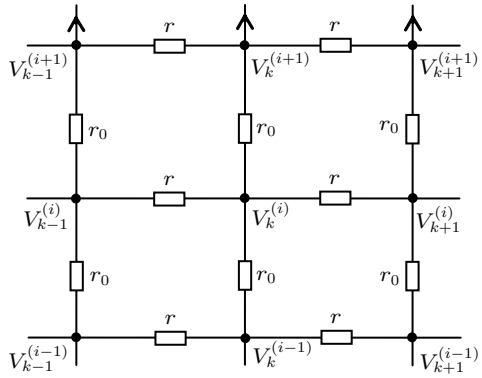

Fig. 2. Resistor sub-network with resistors and potential parameters.

2.3. Two-point resistance

Consider an arbitrary cylindrical $m \times n$ resistor network shown in Fig. 1, where two arbitrary resistors r_1 and r_2 are placed on the left- and right-hand side of the network. The analytic expression of effective resistance between two arbitrary nodes $d_1(x_1,y_1)$ and $d_2(x_2,y_2)$ in the network is given by

$$R_{m\times n}(d_1,d_2) = \frac{|x_2-x_1|}{m}r + \frac{r_0}{2m}\sum_{i=1}^{m-1}\frac{\beta_{1,1}^{(i)} - 2\beta_{1,2}^{(i)}\cos(y\theta_i) + \beta_{2,2}^{(i)}}{(1-\cos\theta_i)G_n^{(i)}}, \quad (11)$$

where $\theta_i = 2i\pi/m$, $y = y_2 - y_1$, $x_1 \leqslant x_2$, and $\beta_{k,s}^{(i)}$ and $G_k^{(i)}$ are, respectively, defined in Eqs. (6) and (7). And $0 \leqslant \{m,n\} \leqslant \infty$, which represent the arbitrary finite and infinite networks, respectively.

The above three main results of Eqs. (8), (10), and (11) are the first finding of this paper, which is a theoretical and technical innovation. Their proofs and applications are given below.

3. Methods and theoretical calculation

RT-V method is pioneered by Tan[43] in 2017. We are going to derive analytic formulae (8), (10), and (11) by using the RT-V method. The derivation of the potential function is a systematic work, including a series of steps, we will derive them through the following five stages.

Stage-1

Building a discrete Poisson equation by the sub-network of Fig. 2. Using Kirchhoff law ($\sum r_i^{-1}V_k = 0$) to establish the voltage equations along the latitude (vertical) direction, we obtain two sets of difference equations for the network of Fig. 1

$$\begin{aligned} V_{k+1}^{(0)} &= (2+2\,h)V_k^{(0)} - V_{k-1}^{(0)} - hV_k^{(m-1)} - hV_k^{(1)}, \\ V_{k+1}^{(i)} &= (2+2\,h)V_k^{(i)} - V_{k-1}^{(i)} - hV_k^{(i-1)} - hV_k^{(i+1)}, \end{aligned} \quad (12)$$

where $h = r/r_0$, and the $i = 0$ in Eq. (12) means that the voltage equation is established on the X axis. The discrete Eq. (12) does not take into account the conditions of the power input node, when the conditions of the power input node (inputing current J at $d_1(x_1,y_1)$ and outputing J at $d_2(x_2,y_2)$) are taken into account, equation (12) can be rewritten as a matrix equation as follows:

$$\boldsymbol{V}_{k+1} = \boldsymbol{B}_m\boldsymbol{V}_k - \boldsymbol{V}_{k-1} - r\boldsymbol{I}_k\delta_{k,x}(\delta_{y,y_1} - \delta_{y,y_2}), \quad (13)$$

where $\delta_{k,k} = 1$ and $\delta_{k,x} = 0$ $(k \neq x)$, and $\boldsymbol{V}_k$ is an $m \times 1$ column matrix, and can be written as

$$\boldsymbol{V}_k = \left[V_k^{(0)},\ V_k^{(1)},\ V_k^{(2)},\ \ldots,\ V_k^{(m-1)}\right]^{\mathrm{T}}, \quad (14)$$

and $\boldsymbol{I}_k$ is

$$\boldsymbol{I}_k = [J,\ J,\ J,\ \ldots,\ J]^{\mathrm{T}}, \quad (15)$$

and $\boldsymbol{B}_m$ is the matrix built along the vertical direction

$$\boldsymbol{B}_m = \begin{pmatrix} 2+2h & -h & 0 & 0 & -h \\ -h & 2(1+h) & -h & 0 & 0 \\ \vdots & \vdots & \ddots & \vdots & \vdots \\ 0 & 0 & -h & 2(1+h) & -h \\ -h & 0 & 0 & -h & 2+2h \end{pmatrix}. \quad (16)$$

Stage-2

Setting up the boundary condition equations on the left and right edges in the network of Fig. 1. Applying the Kirchhoff's law ($\sum r_i^{-1}V_k = 0$) to each boundary of left and right edges, we obtain two matrix equations that relate the left and right boundary as follows:

$$h_1\boldsymbol{V}_1 = [\boldsymbol{B}_m - (2-h_1)\boldsymbol{E}]\boldsymbol{V}_0, \quad (17)$$

$$h_2\boldsymbol{V}_{n-1} = [\boldsymbol{B}_m - (2-h_2)\boldsymbol{E}]\boldsymbol{V}_n, \quad (18)$$

where $h_s = r_s/r_0$ $(s = 1,2)$, $\boldsymbol{E}$ is the $m \times m$ unit matrix, and matrix $\boldsymbol{B}_m$ is given by Eq. (16).

Equations (13)–(18) are all the equations we need in order to derive the potential function. However, we cannot directly solve this equation. In order to solve this difficulty we create new techniques by using the RT theory.[36–38,43] In the following we first give the transform technique, and then give their solution.

Stage-3

Building matrix transform. Firstly, we work out the eigenvalue t_i of matrix $\boldsymbol{B}_m$, solving $\det|\boldsymbol{B}_m - t\boldsymbol{E}| = 0$ to yield

$$t_i = 2(1+h) - 2h\cos\theta_i, \quad (19)$$

where $\theta_i = 2i\pi/m$ $(i = 0,1,2,\ldots m-1)$.

Next, transform Eqs. (13), (17), and (18) by the following methods

$$\boldsymbol{P}_m\boldsymbol{B}_m = \mathrm{diag}\{t_0,t_1,\ldots,t_{m-1}\}\boldsymbol{P}_m, \quad (20)$$

$$\boldsymbol{X}_k = \boldsymbol{P}_m\boldsymbol{V}_k \quad \text{or} \quad \boldsymbol{V}_k = (\boldsymbol{P}_m)^{-1}\boldsymbol{X}_k, \quad (21)$$

where $\boldsymbol{X}_k = \left[X_k^{(0)}, X_k^{(1)}, \ldots, X_k^{(m-1)}\right]^{\mathrm{T}}$. Suggesting that P_i is the row matrix of $\boldsymbol{P}_m$, after rigorous calculation, the P_i can be obtained as follows:

$$P_i = [g_{0,i}, \ g_{1,i}, \ g_{2,i}, \ \ldots, \ g_{m-1,i}], \tag{22}$$

with

$$g_{k,i} = \exp(\mathrm{i}k\theta_i) \quad \text{and} \quad \theta_i = 2i\pi/m, \ (i \geqslant 0), \tag{23}$$

where $\mathrm{i}^2 = -1$. Thus, multiplying Eq. (13) from the left-hand side by $\boldsymbol{P}_m$, we obtain

$$X_{k+1}^{(i)} = t_i X_k^{(i)} - X_{k-1}^{(i)} - rJ(\delta_{x_1,k} g_{y_1,i} - \delta_{x_2,k} g_{y_2,i}), \tag{24}$$

where equations (20) and (21) have been used.

Using a transformation technique similar to the one above, applying $\boldsymbol{P}_m$ to Eqs. (17) and (18), we obtain

$$h_1 X_1^{(i)} = (t_i + h_1 - 2) X_0^{(i)}, \tag{25}$$
$$h_2 X_{n-1}^{(i)} = (t_i + h_2 - 2) X_n^{(i)}. \tag{26}$$

The above equations (19)–(26) are all the transformation equations in order to evaluate the potential.

Stage-4

Solving Eqs. (24)–(26). For solving $X_k^{(i)}$ we should unfold Eq. (24) since it contains several piecewise functions. Thus, we obtain the piecewise solution after solving Eq. (24) as follows:

$$X_k^{(i)} = X_1^{(i)} F_k - X_0^{(i)} F_{k-1}, \quad 0 \leqslant k \leqslant x_1, \tag{27}$$
$$X_{x_1+1}^{(i)} = t_i X_{x_1}^{(i)} - X_{x_1-1}^{(i)} - rJ\exp(\mathrm{i}y_1\theta_i), \tag{28}$$
$$X_k^{(i)} = X_{x_1+1}^{(i)} F_{k-x_1} - X_{x_1}^{(i)} F_{k-x_1-1}, \quad x_1 \leqslant k \leqslant x_2, \tag{29}$$
$$X_{x_2+1}^{(i)} = t_i X_{x_2}^{(i)} - X_{x_2-1}^{(i)} + rJ\exp(\mathrm{i}y_2\theta_i), \tag{30}$$
$$X_k^{(i)} = X_{x_2+1}^{(i)} F_{k-x_2} - X_{x_2}^{(i)} F_{k-x_2-1}, \quad x_2 \leqslant k \leqslant n, \tag{31}$$

where $F_k^{(i)} = (\lambda_i^k - \bar{\lambda}_i^k)/(\lambda_i - \bar{\lambda}_i)$ is defined in Eq. (4), and λ_i and $\bar{\lambda}_i$ are defined in Eq. (3), which are the two roots of the characteristic equation of $\lambda^2 = t_i\lambda - 1$ from Eq. (24).

Please note that we must consider two cases: $i = 0$ and $i \geqslant 1$, because there is $\theta_0 = 0$ ($\theta_i = 2i\pi/m$) if $i = 0$. By Eq. (19) we have the eigenvalue $t_0 = 2$, but $1 - \cos\theta_i$ appears in the denominator of Eqs. (8), (10), and (11). So we need to consider the additional solution of equations when $\theta_0 = 0$.

First we consider the case of $i \geqslant 1$, by Eqs. (25)–(31), we obtain

$$X_k^{(i)} = \frac{\beta_{k\vee x_1}^{(i)} \exp(\mathrm{i}y_1\theta_i) - \beta_{k\vee x_2}^{(i)} \exp(\mathrm{i}y_2\theta_i)}{(t_i - 2)G_n^{(i)}} rJ, \tag{32}$$

where $\beta_{k,s}^{(i)}$ and $G_k^{(i)}$ are, respectively, defined in Eqs. (6) and (7).

Next, we consider the case of $i = 0 \Rightarrow \theta_0 = 0$, by Eqs. (3) and (23), we have

$$\lambda_0 = \bar{\lambda}_0 = 1 \quad \text{and} \quad g_{k,0} = \exp(\mathrm{i}k\theta_0) = 1. \tag{33}$$

Applying limit $\lambda_0 \to 1$ to Eqs. (4) and (5), we have

$$F_k^{(0)} = k, \quad \Delta F_k^{(0)} = 1,$$
$$\alpha_{s,x}^{(0)} = \Delta F_x^{(0)} + (h_s - 1)\Delta F_{x-1}^{(0)} = h_s. \tag{34}$$

In addition, from Eqs. (25) and (26) with $t_0 = 2$, we have

$$X_1^{(0)} = X_0^{(0)}, X_{n-1}^{(0)} = X_n^{(0)}. \tag{35}$$

Substituting Eqs. (33)–(35) into Eqs. (27)–(31), we have

$$X_k^{(0)} = X_0^{(0)}, \quad (0 \leqslant k \leqslant x_1), \tag{36}$$
$$X_{x_1+1}^{(0)} = 2X_{x_1}^{(0)} - X_{x_1-1}^{(0)} - rJ, \tag{37}$$
$$X_k^{(0)} = (k - x_1)X_{x_1+1}^{(0)} - (k - x_1 - 1)X_{x_1}^{(0)}, \quad (x_1 \leqslant k \leqslant x_2), \tag{38}$$
$$X_{x_2+1}^{(0)} = 2X_{x_2}^{(0)} - X_{x_2-1}^{(0)} + rJ, \tag{39}$$
$$X_k^{(0)} = (k - x_2)X_{x_2+1}^{(0)} - (k - x_2 - 1)X_{x_2}^{(0)}, \quad (x_2 \leqslant k \leqslant n). \tag{40}$$

Thus, solving Eqs. (35)–(40), we obtain three solutions below

$$X_k^{(0)} = X_0^{(0)}, \quad 0 \leqslant k \leqslant x_1, \tag{41}$$
$$X_k^{(0)} = X_0^{(0)} + (x_1 - k)\, rJ, \quad x_1 \leqslant k \leqslant x_2, \tag{42}$$
$$X_k^{(0)} = X_0^{(0)} + (x_1 - x_2)\, rJ, \quad x_2 \leqslant k \leqslant n. \tag{43}$$

Obviously, $X_0^{(0)}$ is a constant to be determined, so we use the reference potential to determine the constant of $X_0^{(0)}$.

From Eqs. (21)–(23), we obtain

$$\begin{pmatrix} X_k^{(0)} \\ X_k^{(1)} \\ \vdots \\ X_k^{(s)} \end{pmatrix} = \begin{pmatrix} 1 & 1 & 1 & \ldots & 1 \\ 1 & \exp(\mathrm{i}\theta_1) & \exp(\mathrm{i}2\theta_1) & \ldots & \exp(\mathrm{i}s\theta_1) \\ \vdots & \vdots & \vdots & \ddots & \vdots \\ 1 & \exp(\mathrm{i}\theta_s) & \exp(\mathrm{i}2\theta_s) & \vdots & \exp(\mathrm{i}s\theta_s) \end{pmatrix} \times \begin{pmatrix} V_k^{(0)} \\ V_k^{(1)} \\ \vdots \\ V_k^{(s)} \end{pmatrix}, \tag{44}$$

where $s = m - 1$ (this definition is for simplicity), and $\theta_i = 2i\pi/m$. By Eq. (44) we have

$$X_k^{(0)} = \sum_{i=0}^{m-1} V_k^{(i)}. \tag{45}$$

Since the zero voltage nodes can be assumed and the potential is a scalar relative to a reference point, so we can assume (taking $k = 0$)

$$\sum_{i=0}^{m-1} V_0^{(i)} = 0 \Leftrightarrow X_0^{(0)} = 0. \tag{46}$$

Substituting Eq. (46) into Eqs. (41)–(43), we obtain a unified expression

$$X_k^{(0)} = (x_1 - x_\tau)\, rJ, \quad 0 \leqslant k \leqslant n, \tag{47}$$

where x_τ is defined in Eq. (9). The importance of Eq. (47) should not be underestimated because it is a key solution that it allows us to study resistor networks without relying on the boundary conditions with zero resistance.

In Eq. (46), the sum of the voltages on the left boundary is chosen to be zero, we can also choose the sum of the voltages on the right boundary to be zero, so, equation (45) is used to obtain (taking $k = n$)

$$\sum_{i=0}^{m-1} V_n^{(i)} = 0 \Leftrightarrow X_n^{(0)} = 0, \quad X_0^{(0)} = (x_2 - x_1) rJ. \tag{48}$$

Substituting Eq. (48) into Eqs. (41)–(43), we obtain a unified expression

$$X_k^{(0)} = (x_2 - x_\tau)\, rJ, \quad 0 \leqslant k \leqslant n, \tag{49}$$

where x_τ is defined in Eq. (9).

Stage-5

Using inverse transformation to derive the general formulae (8) and (10). According to the exact calculation, by Eq. (44) we can obtain the inverse transformation equation

$$\begin{pmatrix} V_k^{(0)} \\ V_k^{(1)} \\ \vdots \\ V_k^{(s)} \end{pmatrix} = \frac{1}{m} \begin{pmatrix} 1 & 1 & \cdots & 1 \\ 1 & \exp(-\mathrm{i}\theta_1) & \cdots & \exp(-\mathrm{i}s\theta_s) \\ \vdots & \vdots & \ddots & \vdots \\ 1 & \exp(-\mathrm{i}s\theta_1) & \cdots & \exp(-\mathrm{i}s\theta_s) \end{pmatrix} \times \begin{pmatrix} X_k^{(0)} \\ X_k^{(1)} \\ \vdots \\ X_k^{(s)} \end{pmatrix}, \tag{50}$$

where $s = m - 1$ (this definition is made for simplicity).

Thus, by Eq. (50), we obtain ($y \geqslant 1$)

$$V_k^{(y)} = \frac{1}{m} \left(X_k^{(0)} + \sum_{i=1}^{m-1} X_k^{(i)} \exp(-\mathrm{i}y\theta_i) \right). \tag{51}$$

When taking $\sum_{i=0}^{m-1} V_0^{(i)} = 0$, there is Eq. (47). The substitution of Eqs. (32) and (47) into Eq. (51) yields

$$\frac{U_{m\times n}(x,y)}{J} = \frac{x_1 - x_\tau}{m} r + \frac{r_0}{m} \sum_{i=1}^{m-1} \frac{\beta_{x_1 \vee x}^{(i)} C_{y_1 - y}^{(i)} - \beta_{x_2 \vee x}^{(i)} C_{y_2 - y}^{(i)}}{2(1 - \cos\theta_i) G_n^{(i)}} + \mathrm{i} \frac{r_0}{m} \sum_{i=1}^{m-1} \frac{\beta_{x_1 \vee x}^{(i)} \sin[(y_1 - y)\theta_i] - \beta_{x_2 \vee x}^{(i)} \sin[(y_2 - y)\theta_i]}{2(1 - \cos\theta_i) G_n^{(i)}}. \tag{52}$$

Because the element r_k in the network is a real number, the potential $U(x,y)$ must be a real number. Thus, equation (8) is derived by extracting the real part of Eq. (52).

Again, when taking $\sum_{i=0}^{m-1} V_n^{(i)} = 0$, there is Eq. (49), the substitution of Eqs. (32) and (49) into Eq. (51), then equation (10) is proved.

The above five stages are the specific elaboration of RT-V theory, and can be used to calculate the electrical characteristics of cylindrical networks. Such as stage-1 setting up the main matrix equation, stage-2, setting up the matrix equation with boundary conditions of the left and right edges, stage-3, creating matrix transform, stage-4, solving the matrix equations, and stage-5, deriving the potential by the inverse transform.

Next, we derive Eq. (11). By using Ohm's law, we obtain

$$R_{m\times n}(d_1, d_2) = [U(x_1, y_1) - U(x_2, y_2)] \frac{1}{J}. \tag{53}$$

Using Eq. (8) with $x = \{x_1, x_2\}$ and $y = \{y_1, y_2\}$, we have

$$\frac{U_{m\times n}(x_1, y_1)}{J} = \frac{r_0}{2m} \sum_{i=1}^{m-1} \frac{\beta_{x_1,x_1}^{(i)} - \beta_{x_1,x_2}^{(i)} \cos(y_2 - y_1)\theta_i}{(1 - \cos\theta_i) G_n^{(i)}}, \tag{54}$$

$$\frac{U_{m\times n}(x_2, y_2)}{J} = \frac{x_1 - x_2}{m} r + \frac{r_0}{2m} \sum_{i=1}^{m-1} \frac{\beta_{x_1,x_2}^{(i)} \cos(y_2 - y_1)\theta_i - \beta_{x_2,x_2}^{(i)}}{(1 - \cos\theta_i) G_n^{(i)}}. \tag{55}$$

By Eqs. (54) and (55), we have

$$\frac{U_{m\times n}(x_1, y_1)}{J} - \frac{U_{m\times n}(x_2, y_2)}{J} = \frac{x_2 - x_1}{m} r + \frac{r_0}{m} \sum_{i=1}^{m-1} \left(\frac{\beta_{x_1,x_1}^{(i)} - \beta_{x_1,x_2}^{(i)} \cos(y_2 - y_1)\theta_i}{2(1 - \cos\theta_i) G_n^{(i)}} - \frac{\beta_{x_1,x_2}^{(i)} \cos(y_2 - y_1)\theta_i - \beta_{x_2,x_2}^{(i)}}{2(1 - \cos\theta_i) G_n^{(i)}} \right). \tag{56}$$

Simplifying Eq. (56), together with Eq. (53), we obtain

$$R_{m\times n}(d_1, d_2) = \frac{U_{m\times n}(x_1, y_1)}{J} - \frac{U_{m\times n}(x_2, y_2)}{J} = \frac{x_2 - x_1}{m} r + \frac{r_0}{2m} \sum_{i=1}^{m} \frac{\beta_{x_1,x_1}^{(i)} - 2\beta_{x_1,x_2}^{(i)} \cos(y_2 - y_1)\theta_i + \beta_{x_2,x_2}^{(i)}}{(1 - \cos\theta_i) G_n^{(i)}}. \tag{57}$$

Obviously, from Eq. (57), equation (11) is proved immediately. Similarly, equation (11) can also be proved by Eq. (10), which indicates that the equivalent resistance is independent of the choice of voltage reference point.

In particular, since the RT-V theory is matured, and all results can be strictly calculated by the RT theory. All the calculation processes and conclusions are self-consistent, without any guessing factors, so our results are necessarily correct, and the following special cases verify their correctness again.

4. Applications and discussion

In subsequent sections we consider the applications of formulae to arbitrary lattices. In all applications, we stipulate that all parameters in Eqs. (2)–(7) are applied to all resistor networks, and denote the resistors along the two principal directions by r and r_0 except for resistors on the left-right boundaries, and the input and output node of current are respectively at $d_1(x_1,y_1)$ and $d_2(x_2,y_2)$.

4.1. Applications of potential formula

Formula (8) is a general result because the network of Fig. 1 is very complex and has not been resolved before, which includes a lot of resistor network models, where each of the different boundary resistors represents a different network structure. So formula (8) can create many interesting results.

Application 1 Consider an regular $m\times n$ cylindrical network of Fig. 1 with $r_1=r_2=r_0$, selecting $\sum V_0^{(i)}=0$, by Eq. (8) we have the nodal potential as follows:

$$\frac{U(x,y)}{J}=\frac{x_1-x_\tau}{m}r+\frac{r_0}{2m}\sum_{i=1}^{m-1}\frac{\beta_{x_1\vee x}^{(i)}C_{y_1-y}^{(i)}-\beta_{x_2\vee x}^{(i)}C_{y_2-y}^{(i)}}{(1-\cos\theta_i)F_{n+1}^{(i)}}, \quad (58)$$

where $\beta_{x\vee x_k}^{(i)}$ reduces to $\beta_{x,x_s}^{(i)}=\Delta F_x^{(i)}\Delta F_{n-x_s}^{(i)}$.

Application 2 Consider a non-regular $m\times n$ cylindrical network as shown in Fig. 1. Defining $C_{y_k-y}^{(i)}=\cos(y_k-y)\theta_i$ with $\theta_i=2i\pi/m$, and selecting $\sum V_0^{(i)}=0$, when $x_2=x_1$, the potential of any node $d(x,y)$ in the finite and sem-infinite networks can be written respectively as

$$\frac{U_{m\times n}(x,y)}{J}=\frac{r_0}{2m}\sum_{i=1}^{m-1}\frac{C_{y_1-y}^{(i)}-C_{y_2-y}^{(i)}}{(1-\cos\theta_i)G_n^{(i)}}\beta_{x_1\vee x}^{(i)}, \quad (59)$$

$$\frac{U_{m\times\infty}(x,y)}{J}=\frac{r}{2m}\sum_{i=1}^{m-1}\frac{C_{y_1-y}^{(i)}-C_{y_2-y}^{(i)}}{\sqrt{(1+h-h\cos\theta_i)^2-1}}\bar{\lambda}_i^{|x_1-x|}. \quad (60)$$

Here, equation (60) is generated by taking the limit of Eq. (59) when $n\to\infty$ and $x_1\to\infty$.

Application 3 Consider an $m\times n$ cylindrical network of Fig. 1. When $r_2=0$, figure 1 degrades into a cobweb network as shown in Fig. 3. Selecting $\sum V_0^{(i)}=0$ as the reference potential, by Eq. (8) we have the nodal potential

$$\frac{U(x,y)}{J}=\frac{x_1-x_\tau}{m}r+\frac{r}{m}\sum_{i=1}^{m-1}\frac{\beta_{x_1\vee x}^{(i)}C_{y_1-y}^{(i)}-\beta_{x_2\vee x}^{(i)}C_{y_2-y}^{(i)}}{\Delta F_n^{(i)}+(h_1-1)\Delta F_{n-1}^{(i)}}, \quad (61)$$

where $\beta_{x_s\vee x}^{(i)}$ is redefined as $\beta_{x\vee x_s}^{(i)}=\alpha_{1,x}^{(i)}F_{n-x_s}^{(i)}$ (if $x\leqslant x_s$) and $\beta_{x\vee x_s}^{(i)}=\alpha_{1,x_s}^{(i)}F_{n-x}^{(i)}$ (if $x\geqslant x_s$).

In particular, when $d_1(0,y_1)$ is on the left edge, and $d_2(n,y_2)$ is on the right edge, equation (61) reduces to

$$\frac{U(x,y)}{J}=-\frac{x}{m}r+\frac{r_1h}{m}\sum_{i=1}^{m-1}\frac{F_{n-x}^{(i)}\cos(y_1-y)\theta_i}{\Delta F_n^{(i)}+(h_1-1)\Delta F_{n-1}^{(i)}}. \quad (62)$$

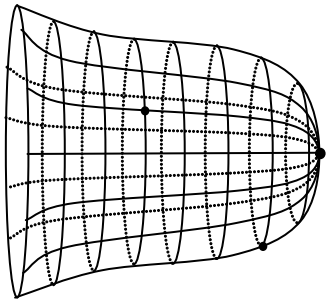

Fig. 3. $m\times n$ cobweb network with arbitrary left boundary resistor of r_1.

Application 4 Consider an $m\times n$ resistor network of Fig. 1. When $r_2=0$, figure 1 degrades into a cobweb network as shown in Fig. 3. Selecting $\sum V_n^{(i)}=0$ as the reference potential, by Eq. (10) we have the nodal potential

$$\frac{U(x,y)}{J}=\frac{x_2-x_\tau}{m}r+\frac{r}{m}\sum_{i=1}^{m-1}\frac{\beta_{x_1\vee x}^{(i)}C_{y_1-y}^{(i)}-\beta_{x_2\vee x}^{(i)}C_{y_2-y}^{(i)}}{\Delta F_n^{(i)}+(h_1-1)\Delta F_{n-1}^{(i)}}, \quad (63)$$

where $\beta_{x_s\vee x}^{(i)}$ is exactly the same as $\beta_{x_s\vee x}^{(i)}$ appearing in Eq. (61).

In particular, when $d_1(0,y_1)$ is on the left edge, and $d_2(n,y_2)$ is on the right edge, equation (63) reduces to

$$\frac{U(x,y)}{J}=\frac{n-x}{m}r+\frac{r_1h}{m}\sum_{i=1}^{m-1}\frac{F_{n-x}^{(i)}\cos(y_1-y)\theta_i}{\Delta F_n^{(i)}+(h_1-1)\Delta F_{n-1}^{(i)}}. \quad (64)$$

Please note that the cobweb network with an arbitrary boundary has not been resolved before, in previous work only the normal cobweb network (the boundary resistor is $r_1=r_0$) was studied.[43] So, equations (61) and (63) are two original results.

Application 5 Consider an arbitrary $m\times n$ globe network as shown in Fig. 4. That is to say, figure 1 degrades into a globe network when $r_1=r_2=0$. Selecting $\sum V_0^{(i)}=0$, from Eq. (8) we have the nodal potential

$$\frac{U_{m\times n}(x,y)}{J}=\frac{x_1-x_\tau}{m}r+\frac{r}{m}\sum_{i=1}^{m-1}\frac{\beta_{x_1\vee x}^{(i)}C_{y_1-y}^{(i)}-\beta_{x_2\vee x}^{(i)}C_{y_2-y}^{(i)}}{F_n^{(i)}}, \quad (65)$$

where we redefine $\beta_{x\vee x_s}^{(i)}=F_x^{(i)}F_{n-x_s}^{(i)}$ (if $x\leqslant x_s$) and $\beta_{x\vee x_s}^{(i)}=F_{x_s}^{(i)}F_{n-x}^{(i)}$ (if $x\geqslant x_s$).

In particular, when $d_1(0,y_1)$ is at the left pole, and $d_2(n,y_2)$ is at the right pole, equation (65) reduces to

$$\frac{U(x,y)}{J} = -\frac{x}{m}r. \tag{66}$$

Formula (66) satisfies $U(0,0)=0$, which is very simple and very interesting because the potential distribution is only related to the x and unrelated to y, and shows the nodal potential is equal in the same latitude.

In addition, when $d_1(0,y_1)$ is at the left pole, and $d_2(n,y_2)$ is at the right pole, and $r_1=r_2=0$, selecting $\sum V_n^{(i)}=0$, by Eq. (10) we have the nodal potential as follows:

$$\frac{U(x,y)}{J} = \frac{x}{m}r. \tag{67}$$

Theoretical formulae (8), (10), and (11) are three universal formulae, relatively esoteric, which contain a variety of conditions, wide application, far-reaching significance. The following simple examples will help the readers further understand the meaning of formula (8).

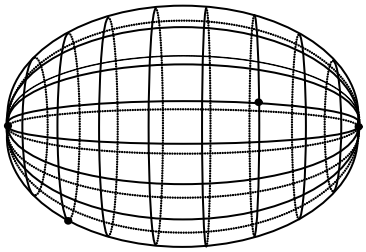

Fig. 4. Arbitrary $m\times n$ globe network, where m and n are the number of grids along the cycle direction and horizontal direction respectively, with the resistors r and r_0 in horizontal direction and loop direction, respectively.

Application 6 When $m=4$, figure 2 degrades into a 3D $\square\times n$ resistor network as shown in Fig. 5. By Eq. (2) we have $\theta_i = i\pi/2$, and substituting it into Eq. (3) yields

$$\begin{aligned}\lambda_1 &= \lambda_3 = 1+h+\sqrt{(1+h)^2-1},\\ \lambda_2 &= 1+2h+\sqrt{(1+2\,h)^2-1}.\end{aligned} \tag{68}$$

So we have $\beta_{t,s}^{(3)}=\beta_{t,s}^{(1)}$, $G_n^{(3)}=G_n^{(1)}$, $\theta_1=\pi/2$, and $\theta_2=\pi$. Assume that the input current J is at $A_{x_1}(x_1,0)$, and the output current J is at $P_{x_2}(x_2,y_2)$, where P_k represents the nodes of A_k, B_k, C_k, and D_k, and $V_{A_0}+V_{B_0}+V_{C_0}+V_{D_0}=0$ is selected. By Eq. (8), we have the nodal potential

$$\begin{aligned}\frac{U_{\square\times n}(x,y)}{J} &= \frac{x_1-x_\tau}{4}r + r_0\frac{\beta_{x_1\vee x}^{(1)}C_y^{(1)}-\beta_{x_2\vee x}^{(1)}C_{y_2-y}^{(1)}}{4G_n^{(1)}}\\ &\quad + r_0\frac{\beta_{x_1\vee x}^{(2)}C_y^{(2)}-\beta_{x_2\vee x}^{(2)}C_{y_2-y}^{(2)}}{16G_n^{(2)}},\end{aligned} \tag{69}$$

where $C_{y_k-y}^{(i)}=\cos[(y_k-y)i\pi/2]$ and x_τ is defined in Eq. (9).

It is not hard to see that Eq. (69) is still quite profound in terms of understanding its physical meaning. Since the node potential value is related to the input position of the power source, different input positions of the power supply will generate different potential values. To understand the nature of the problem easily, we list the following five cases.

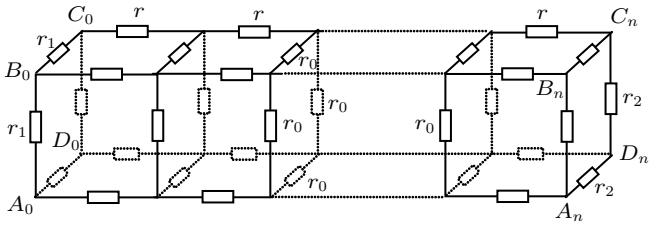

Fig. 5. 3D $\square\times n$ network with resistors r and r_0 in respective horizontal and vertical directions except for r_1 and r_2 on the left and right edges.

Case-1 Assume that the input current J is at $A_0(0,0)$ and the output current J is at $B_0(0,1)$, and select $V_{A_0}+V_{B_0}=0$, then by Eq. (69) we will have the nodal potential

$$\begin{aligned}\frac{U_{\square\times n}(x,y)}{J} &= r_1\frac{C_y^{(1)}-C_{1-y}^{(1)}}{4G_n^{(1)}}\alpha_{2,n-x}^{(1)}\\ &\quad + r_1\frac{C_y^{(2)}-C_{1-y}^{(2)}}{16G_n^{(2)}}\alpha_{2,n-x}^{(2)},\end{aligned} \tag{70}$$

where $C_{k-y}^{(i)}=\cos[(k-y)i\pi/2]$, $\alpha_{2,n-x}^{(i)}=\Delta F_{n-x}^{(i)}+(h_2-1)\Delta F_{n-x-1}^{(i)}$. However, equation (70) still contains multiple results, such as the nodal potential on different axes

$$\frac{U_{\square\times n}(A_x)}{J} = r_1\frac{\alpha_{2,n-x}^{(1)}}{4G_n^{(1)}}+r_1\frac{\alpha_{2,n-x}^{(2)}}{8G_n^{(2)}}, \tag{71}$$

$$U_{\square\times n}(B_x) = -U_{\square\times n}(A_x), \tag{72}$$

$$\frac{U_{\square\times n}(C_x)}{J} = -r_1\frac{\alpha_{2,n-x}^{(1)}}{4G_n^{(1)}}+r_1\frac{\alpha_{2,n-x}^{(2)}}{8G_n^{(2)}}, \tag{73}$$

$$U_{\square\times n}(D_x) = -U_{\square\times n}(C_x). \tag{74}$$

Equations (72) and (74) reveal the physical meaning. Since the input positions of the power source are at $A_0(0,0)$ and $B_0(0,1)$ together with the assumption of $V_{A_0}+V_{B_0}=0$, we have $U_{\square\times n}(A_x)+U_{\square\times n}(B_x)=0$ and $U_{\square\times n}(D_x)=-U_{\square\times n}(C_x)$. This shows that the potential of symmetric nodes has symmetry, which is completely consistent with the actual situation.

Case-2 Assume that the input current J is at $A_0(0,0)$, and the output current J is at $C_0(0,2)$, and select $V_{A_0}+V_{C_0}=0$ as the reference potential, then by Eq. (69) we will have the nodal potential

$$\begin{aligned}\frac{U_{\square\times n}(x,y)}{J} &= r_1\frac{C_y^{(1)}-C_{2-y}^{(1)}}{4G_n^{(1)}}\alpha_{2,n-x}^{(1)}\\ &\quad + r_1\frac{C_y^{(2)}-C_{2-y}^{(2)}}{16G_n^{(2)}}\alpha_{2,n-x}^{(2)},\end{aligned} \tag{75}$$

where $C_{k-y}^{(i)}=\cos[(k-y)i\pi/2]$. However, equation (75) still

contains multiple results, such as the nodal potential on different axes

$$\frac{U_{\square\times n}(A_x)}{J} = r_1\frac{\alpha^{(1)}_{2,n-x}}{2G^{(1)}_n}, \tag{76}$$

$$U_{\square\times n}(B_x) = U_{\square\times n}(D_x) = 0, \tag{77}$$

$$U_{\square\times n}(C_x) = -U_{\square\times n}(A_x). \tag{78}$$

Equations (76)–(78) reveal the physical meaning. Because axis A_0A_n and axis C_0C_n are symmetric in Fig. 5, clearly, when selecting $V_{A_0}+V_{C_0}=0$, there is $U_{\square\times n}(A_x)+U_{\square\times n}(C_x)=0$ which satisfies Eq. (78), shows that the potential of symmetric nodes has symmetry.

Case-3 Assume that the input current is at $A_0(0,0)$, and the output current is at $A_n(n,0)$, and select $V_{A_0}+V_{B_0}+V_{C_0}+V_{D_0}=0$ as the reference potential, then by Eq. (69) we will have the nodal potential

$$\frac{U_{\square\times n}(x,y)}{J} = -\frac{x}{4}r + r_0\frac{h_1\alpha^{(1)}_{2,n-x}-h_2\alpha^{(1)}_{1,x}}{4G^{(1)}_n}C^{(1)}_y + r_0\frac{h_1\alpha^{(2)}_{2,n-x}-h_2\alpha^{(2)}_{1,x}}{16G^{(2)}_n}C^{(2)}_y, \tag{79}$$

where $h_k=r_k/r_0$ and $C^{(i)}_y=\cos(yi\pi/2)$. However, equation (79) still contains multiple results, such as

$$\frac{U_{\square\times n}(A_x)}{J} = -\frac{x}{4}r + r_0\frac{h_1\alpha^{(1)}_{2,n-x}-h_2\alpha^{(1)}_{1,x}}{4G^{(1)}_n} + r_0\frac{h_1\alpha^{(2)}_{2,n-x}-h_2\alpha^{(2)}_{1,x}}{16G^{(2)}_n}, \tag{80}$$

$$\frac{U_{\square\times n}(B_x)}{J} = \frac{U_{\square\times n}(D_x)}{J} = -\frac{x}{4}r - r_0\frac{h_1\alpha^{(2)}_{2,n-x}-h_2\alpha^{(2)}_{1,x}}{16G^{(2)}_n}, \tag{81}$$

$$\frac{U_{\square\times n}(C_x)}{J} = -\frac{x}{4}r - r_0\frac{h_1\alpha^{(1)}_{2,n-x}-h_2\alpha^{(1)}_{1,x}}{4G^{(1)}_n} + r_0\frac{h_1\alpha^{(2)}_{2,n-x}-h_2\alpha^{(2)}_{1,x}}{16G^{(2)}_n}. \tag{82}$$

Obviously, according to the symmetry of node potential, equation (81) is completely consistent with the actual situation. In addition, we find that $U_{\square\times n}(A_x)+2U_{\square\times n}(B_x)+U_{\square\times n}(C_x)=-xrJ$, which is interesting and shows that we can obtain another node potential if we obtain two of the three results of $U_{\square\times n}(A_x)$, $U_{\square\times n}(B_x)$, and $U_{\square\times n}(C_x)$.

Case-4 Assume that the input current is at $A_0(0,0)$, and the output current is at $B_n(n,1)$, and select $V_{A_0}+V_{B_0}+V_{C_0}+V_{D_0}=0$ as the reference potential, then by Eq. (69) we will have the nodal potential

$$\frac{U_{\square\times n}(x,y)}{J} = -\frac{x}{4}r + r_0\frac{h_1\alpha^{(1)}_{2,n-x}C^{(1)}_y-h_2\alpha^{(1)}_{1,x}C^{(1)}_{1-y}}{4G^{(1)}_n} + r_0\frac{h_1\alpha^{(2)}_{2,n-x}C^{(2)}_y-h_2\alpha^{(2)}_{1,x}C^{(2)}_{1-y}}{16G^{(2)}_n}, \tag{83}$$

where $h_k=r_k/r_0$ and $C^{(i)}_{k-y}=\cos[(k-y)i\pi/2]$. However, equation (83) still contains multiple results, such as

$$\frac{U_{\square\times n}(A_x)}{J} = -\frac{x}{4}r + r_1\frac{\alpha^{(1)}_{2,n-x}}{4G^{(1)}_n} + r_0\frac{h_1\alpha^{(2)}_{2,n-x}+h_2\alpha^{(2)}_{1,x}}{16G^{(2)}_n}, \tag{84}$$

$$\frac{U_{\square\times n}(B_x)}{J} = -\frac{x}{4}r - r_2\frac{\alpha^{(1)}_{1,x}}{4G^{(1)}_n} - r_0\frac{h_1\alpha^{(2)}_{2,n-x}+h_2\alpha^{(2)}_{1,x}}{16G^{(2)}_n}, \tag{85}$$

$$\frac{U_{\square\times n}(C_x)}{J} = -\frac{x}{4}r - r_1\frac{\alpha^{(1)}_{2,n-x}}{4G^{(1)}_n} + r_0\frac{h_1\alpha^{(2)}_{2,n-x}+h_2\alpha^{(2)}_{1,x}}{16G^{(2)}_n}, \tag{86}$$

$$\frac{U_{\square\times n}(D_x)}{J} = -\frac{x}{4}r + r_2\frac{\alpha^{(1)}_{1,x}}{4G^{(1)}_n} - r_0\frac{h_1\alpha^{(2)}_{2,n-x}+h_2\alpha^{(2)}_{1,x}}{16G^{(2)}_n}. \tag{87}$$

Case-5 Assume that the input current is at $A_0(0,0)$, and the output current is at $C_n(n,3)$, and select $V_{A_0}+V_{B_0}+V_{C_0}+V_{D_0}=0$ as the reference potential, then by Eq. (69) we will have the nodal potential

$$\frac{U_{\square\times n}(x,y)}{J} = -\frac{x}{4}r + r_0\frac{h_1\alpha^{(1)}_{2,n-x}C^{(1)}_y-h_2\alpha^{(1)}_{1,x}C^{(1)}_{2-y}}{4G^{(1)}_n} + r_0\frac{h_1\alpha^{(2)}_{2,n-x}C^{(2)}_y-h_2\alpha^{(2)}_{1,x}C^{(2)}_{2-y}}{16G^{(2)}_n}, \tag{88}$$

where $h_k=r_k/r_0$ and $C^{(i)}_{k-y}=\cos[(k-y)i\pi/2]$. However, equation (88) still contains multiple results, such as

$$\frac{U_{\square\times n}(A_x)}{J} = -\frac{x}{4}r + r_0\frac{h_1\alpha^{(1)}_{2,n-x}+h_2\alpha^{(1)}_{1,x}}{4G^{(1)}_n} + r_0\frac{h_1\alpha^{(2)}_{2,n-x}-h_2\alpha^{(2)}_{1,x}}{16G^{(2)}_n}, \tag{89}$$

$$\frac{U_{\square\times n}(B_x)}{J} = \frac{U_{\square\times n}(D_x)}{J} = -\frac{x}{4}r - r_0\frac{h_1\alpha^{(2)}_{2,n-x}-h_2\alpha^{(2)}_{1,x}}{16G^{(2)}_n}, \tag{90}$$

$$\frac{U_{\square\times n}(C_x)}{J} = -\frac{x}{4}r - r_0\frac{h_1\alpha^{(1)}_{2,n-x}+h_2\alpha^{(1)}_{1,x}}{4G^{(1)}_n} + r_0\frac{h_1\alpha^{(2)}_{2,n-x}-h_2\alpha^{(2)}_{1,x}}{16G^{(2)}_n}. \tag{91}$$

Obviously, according to the symmetry of node potential, equation (90) is completely consistent with the actual situation.

The above series of results (69)–(91) is the first to be found in this paper, which basically explain the basic meaning of formula (8) and can effectively help readers understand and use formula (8).

4.2. Applications of resistance formula

Formula (11) is a precise and profound result since the network of Fig. 1 is very complex and has not been resolved before and includes a lot of resistor network models, where each of the different boundary resistor r_i represents a different

network structure. In particular, taking some specific values of r_1 and r_2, and assuming $x_1 \leqslant x_2$, equation (11) gives rise to a series of special cases below.

Case A When $r_1 = r_2 = r_0$, figure 1 degrades into a normal $m \times n$ cylindrical network, then the resistance of Eq. (11) reduces to

$$R_{m\times n}(d_1,d_2) = \frac{|x_2-x_1|}{m}r + \frac{r_0}{2m}\sum_{i=1}^{m-1}\frac{\beta_{1,1}^{(i)} - 2\beta_{1,2}^{(i)}\cos(y\theta_i) + \beta_{2,2}^{(i)}}{(1-\cos\theta_i)F_{n+1}^{(i)}}, \quad (92)$$

where $\beta_{k,s}^{(i)}$ reduces to $\beta_{k,s}^{(i)} = \Delta F_{x_k}^{(i)}\Delta F_{n-x_s}^{(i)}$, and $y = y_1 - y_2$. The normal cylindrical network has been studied in Ref. [26], leading to Eq. (1) with a double sum. Obviously, our result (92) is different from Eq. (1). This shows that the effective resistance can be expressed in different forms for the same resistor network.

Case B Consider a non-regular $m \times n$ cylindrical network of Fig. 1, when $r_1 = r_0$ and r_2 is an arbitrary resistor, the resistance of Eq. (11) reduces to

$$R_{m\times n}(d_1,d_2) = \frac{|x_2-x_1|}{m}r + \frac{r_0}{2m}\sum_{i=1}^{m-1}\frac{\beta_{1,1}^{(i)} - 2\beta_{1,2}^{(i)}\cos(y\theta_i) + \beta_{2,2}^{(i)}}{(1-\cos\theta_i)[F_{n+1}^{(i)} + (h_2-1)F_n^{(i)}]}, \quad (93)$$

where $\beta_{k,s}^{(i)}$ reduces to $\beta_{k,s}^{(i)} = \Delta F_{x_k}^{(i)}[\Delta F_{n-x_s}^{(i)} + (h_2-1)\Delta F_{n-x_s-1}^{(i)}]$, and $\theta_i = 2i\pi/m$, $y = y_2 - y_1$.

Case C When $r_2 = 0$, the right boundary of Fig. 1 collapses to a pole, so the non-regular cylindrical network degrades into a cobweb network with an arbitrary boundary resistor r_1 as shown in Fig. 3. By Eq. (11) we obtain the resistance formula

$$R_{m\times n}(d_1,d_2) = \frac{|x_2-x_1|}{m}r + \frac{r}{m}\sum_{i=1}^{m-1}\frac{\beta_{1,1}^{(i)} - 2\beta_{1,2}^{(i)}\cos(y\theta_i) + \beta_{2,2}^{(i)}}{\Delta F_n^{(i)} + (h_1-1)\Delta F_{n-1}^{(i)}}, \quad (94)$$

where $\beta_{k,s}^{(i)}$ is re-defined as $\beta_{k,s}^{(i)} = [\Delta F_{x_k}^{(i)} + (h_1-1)\Delta F_{x_k-1}^{(i)}]F_{n-x_s}^{(i)}$.

In particular, selecting $h_1 = 1$ and $h_2 = 0$, the resistor network of Fig. 3 degrades into a regular cobweb network, the resistance of Eq. (94) reduces to

$$R_{m\times n}(d_1,d_2) = \frac{|x_2-x_1|}{m}r + \frac{r}{m}\sum_{i=1}^{m-1}\frac{\beta_{1,1}^{(i)} - 2\beta_{1,2}^{(i)}\cos(y\theta_i) + \beta_{2,2}^{(i)}}{\Delta F_n^{(i)}}, \quad (95)$$

where $\beta_{k,s}^{(i)}$ is redefined as $\beta_{k,s}^{(i)} = \Delta F_{x_k}^{(i)}F_{n-x_s}^{(i)}$.

Please note that the regular cobweb network was studied in Refs. [28] and [35] but the results in Refs. [28] and [35] are different from those from Eq. (95). That is because reference [35] chooses the coordinates in different directions to set up the matrix equations, where reference [35] set up matrix along the longitude, but this paper sets up matrix along the latitude, and reference [28] studied the problem by the WU's method which gives the result in double sum.

Case D When $h_1 = h_2 = 0$ ($r_1 = r_2 = 0$), the left and right boundaries collapse respectively to two poles, the network of Fig. 1 degrades into an $m \times n$ globe network as shown in Fig. 4, by Eq. (11) we have

$$R_{m\times n}(d_1,d_2) = \frac{|x_2-x_1|}{m}r + \frac{r}{m}\sum_{i=1}^{m-1}\frac{F_{x_1}^{(i)}F_{n-x_1}^{(i)} - 2F_{x_1}^{(i)}F_{n-x_2}^{(i)}\cos(y\theta_i) + F_{x_2}^{(i)}F_{n-x_2}^{(i)}}{F_n^{(i)}}, \quad (96)$$

where $y = y_1 - y_2$ and $\theta_i = 2i\pi/m$.

Please note that the globe network was studied in Ref. [34], but the result in Ref. [34] is different from that from Eq. (96). That is because they chose coordinates in different directions to set up the matrix equations, which implies that the effective resistance can be expressed in different forms for the same resistor network.

Case E Consider a complex $m \times n$ cylindrical network of Fig. 1, when $d_1(0,0)$ is on the left edge and $d_2(n,y)$ is on the right edge, the resistance between two edges is

$$R_{m\times n}(\{0,0\},\{n,y\}) = \frac{n}{m}r + \frac{r_0}{2m}\sum_{i=1}^{m-1}\frac{h_1\alpha_{2,n}^{(i)} + h_2\alpha_{1,n}^{(i)} - 2h_1h_2\cos(y\theta_i)}{(1-\cos\theta_i)G_n^{(i)}}. \quad (97)$$

In particular, when $h_1 = h_2 = 1$, equation (97) reduces to

$$R_{m\times n}(\{0,0\},\{n,y\}) = \frac{n}{m}r + \frac{r_0}{m}\sum_{i=1}^{m-1}\frac{\Delta F_n^{(i)} - \cos(y\theta_i)}{(1-\cos\theta_i)F_{n+1}^{(i)}}. \quad (98)$$

When $h_1 = 0$ and $h_2 = 1$, equation (97) reduces to

$$R_{m\times n}(\{0,0\},\{n,y\}) = \frac{n}{m}r + \frac{r}{m}\sum_{i=1}^{m-1}\frac{F_n^{(i)}}{\Delta F_n^{(i)}}. \tag{99}$$

Case F Consider a complex $m \times n$ cylindrical network of Fig. 1, when both $d_1(x_1,0)$ and $d_2(x_2,0)$ are on the same horizontal axis, we have

$$R_{m\times n}(\{x_1,0\},\{x_2,0\}) = \frac{|x_2-x_1|}{m}r + \frac{r_0}{2m}\sum_{i=1}^{m-1}\frac{\beta_{1,1}^{(i)} - 2\beta_{1,2}^{(i)} + \beta_{2,2}^{(i)}}{(1-\cos\theta_i)G_n^{(i)}}. \tag{100}$$

It is essential to take formula (11) into account again in order to help the readers further understand its meaning, here three simple examples are given below.

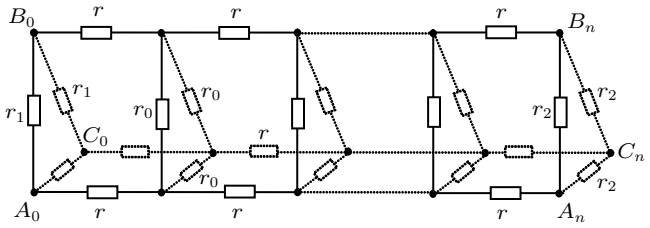

Fig. 6. 3D $\Delta \times n$ network with resistors r and r_0 in the respective horizontal and vertical directions except for r_1 and r_2 on the left and right edges.

Case G When $m = 3$, figure 1 degrades into a 3D $\Delta \times n$ resistor network as shown in Fig. 6. By $\theta_i = 2i\pi/m$ we have $\theta_i = 2i\pi/3$ $(i = 1,2)$, substituting them into Eq. (3) yields

$$\lambda_1 = \lambda_2 = 1 + \frac{3}{2}h + \sqrt{\left(1+\frac{3}{2}h\right)^2 - 1}. \tag{101}$$

So, we have $\beta_{t,s}^{(2)} = \beta_{t,s}^{(1)}$, $\theta_1 = 2\pi/3$, and $\theta_2 = 4\pi/3$. By Eq. (11), we obtain the resistance formula between any two nodes

$$R_{\Delta\times n}(A_{x_1},P_k) = \frac{|k-x_1|}{3}r + \frac{2r_0}{9}\left(\frac{\beta_{1,1}^{(1)} - 2\beta_{1,2}^{(1)}\cos(2\pi y/3) + \beta_{2,2}^{(1)}}{G_n^{(1)}}\right), \tag{102}$$

where P_k represents the nodes of A_k, B_k, C_k, and $\beta_{k,s}^{(1)}$ and $G_k^{(1)}$ are, respectively, defined in Eqs. (6) and (7).

Please note that figure 6 is a new model since the boundary resistors of r_1 and r_2 are two arbitrary values which can lead to different geometries. In Ref. [33] studied is only the network of canonical structure of $r_1 = r_2 = r_0$. So, equation (102) is a general formula, which can produce several specific results below.

Considering the resistance between two nodes A_{x_1} and A_{x_2}, there be $y = 0$ and equation (102) reduces to

$$R_{\Delta\times n}(A_{x_1},A_{x_2}) = \frac{|x_2-x_1|}{3}r + \frac{2r_0}{9}\left(\frac{\beta_{x_1,x_1}^{(1)} - 2\beta_{x_1,x_2}^{(1)} + \beta_{x_2,x_2}^{(1)}}{G_n^{(1)}}\right), \tag{103}$$

where $\beta_{x_1,k}^{(i)} = \alpha_{1,x_1}^{(i)}\alpha_{2,n-k}^{(i)}$ is defined in Eq. (6).

In particular, when $x_1 = 0$ and $r_1 = r_2 = r_0$, equation (103) reduces to

$$R_{\Delta\times n}(A_0,A_x) = \frac{x}{3}r + \frac{2r_0}{9}\left(\frac{\Delta F_n^{(1)} - 2\Delta F_{n-x}^{(1)} + \Delta F_x^{(1)}\Delta F_{n-x}^{(1)}}{F_{n+1}^{(1)}}\right), \tag{104}$$

$$R_{\Delta\times n}(A_0,A_n) = \frac{n}{3}r + \frac{4r_0}{9}\left(\frac{\Delta F_n^{(1)} - 1}{F_{n+1}^{(1)}}\right). \tag{105}$$

Considering the resistance between two nodes A_{x_1} and B_k (or C_k), there is $y = 1$, and equation (102) reduces to

$$R_{\Delta\times n}(A_{x_1},B_k) = R_{\Delta\times n}(A_{x_1},C_k) = \frac{|k-x_1|}{3}r + \frac{2r_0}{9}\left(\frac{\beta_{1,1}^{(1)} + \beta_{1,2}^{(1)} + \beta_{2,2}^{(1)}}{G_n^{(1)}}\right). \tag{106}$$

In particular, when $x_1 = 0$ and $r_1 = r_2 = r_0$, equation (106) reduces to

$$R_{\Delta\times n}(A_0,B_k) = R_{\Delta\times n}(A_0,C_k) = \frac{k}{3}r + \frac{2r_0}{9}\left(\frac{\Delta F_n^{(1)} + \Delta F_{n-k}^{(1)} + \Delta F_k^{(1)}\Delta F_{n-k}^{(1)}}{F_{n+1}^{(1)}}\right), \tag{107}$$

$$R_{\Delta\times n}(A_0,B_n) = R_{\Delta\times n}(A_0,C_n) = \frac{n}{3}r + 2r_0\frac{2\Delta F_n^{(1)} + 1}{9F_{n+1}^{(1)}}. \tag{108}$$

When $x_1 = k$ and $r_1 = r_2 = r_0$, from Eq. (106) we have

$$R_{\Delta\times n}(A_k, B_k) = R_{\Delta\times n}(A_k, C_k) = 2r_0 \frac{\Delta F_k^{(1)} \Delta F_{n-k}^{(1)}}{3F_{n+1}^{(1)}}. \quad (109)$$

Figure 6 is a simple and common network model, but due to the complexity of the boundary conditions, it is always difficult to obtain equivalent resistance. Equation (102) is given for the first time, which provides a new theoretical basis for practical application.

In order to clearly understand the change rule of equivalent resistances $R_{\Delta\times n}(A_0, A_k)$ and $R_{\Delta\times n}(A_0, B_k)$, we use Matlab to draw their change curve as shown in Figs. 7–9.

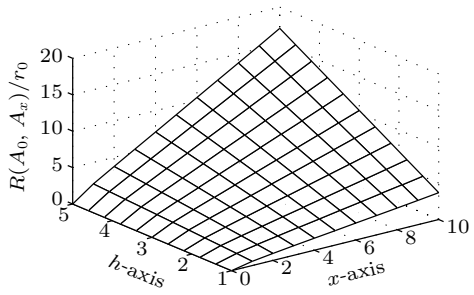

Fig. 7. 3D graph showing equivalent resistance $R(A_0, A_k)$ changing with h and x in $\Delta \times n$ network, and resistance $R(A_0, A_x)$ increasing with augment of n and x, where $R(A_0, A_0) = 0$ when $x = 0$.

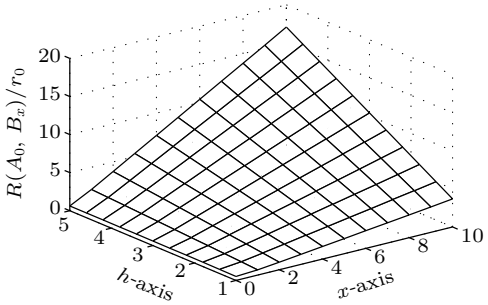

Fig. 8. 3D graph showing equivalent resistance $R(A_0, B_k)$ changing with h and x in $\Delta \times n$ network, and the resistance $R(A_0, B_x)$ increasing with argument of n and x, where $R(A_0, B_0) > 0$ when $x = 0$.

Comparing Fig. 7 with Fig. 8, we find that their variation patterns are basically similar, but there are slight differences between them, that is, $R_{\Delta\times n}(A_0, A_0) = 0$ and $R_{\Delta\times n}(A_0, B_0) > 0$ which are exactly the same as the results of the actual circuit. The equivalent resistance $R(A_0, B_k)$ increases with n and x increasing. Figure 9 shows that $R(A_0, B_0)$ decreases with the increase of n, but $R(A_0, B_0)$ increases with h increasing except for $n = 0$. Since our formulae are all accurate and not estimates, all the computer simulation results are exactly the same as those in the three figures, *i.e.*, Figs. 7–9, which indirectly indicates the correctness of our results.

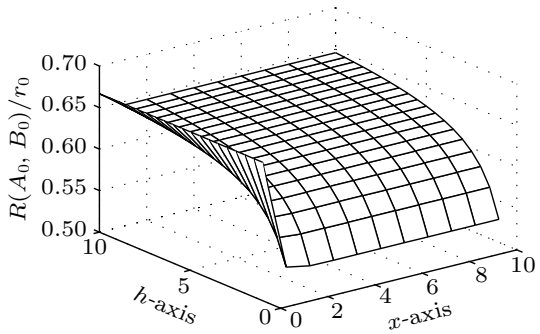

Fig. 9. 3D graph showing equivalent resistance $R(A_0, B_0)$ changing with h and n in $\Delta \times n$ network, $R(A_0, B_0)$ decreasing with the increase of n, and $R(A_0, B_0)$ increasing with argument of h except for $n = 0$.

Case H When $m = 4$, figure 2 degrades into a 3D $\square \times n$ resistor network as shown in Fig. 5. We can obtain the equivalent resistance between any two nodes by Eq. (11). Firstly, by Eq. (2) we have $\theta_i = i\pi/2$, substituting it into Eq. (3) yields

$$\begin{aligned} \lambda_1 &= \lambda_3 = 1 + h + \sqrt{h^2 + 2h}, \\ \lambda_2 &= 1 + 2h + 2\sqrt{h^2 + h}. \end{aligned} \quad (110)$$

So we have $\beta_{t,s}^{(3)} = \beta_{t,s}^{(1)}$, $\theta_1 = \pi/2$, and $\theta_2 = \pi$. By Eq. (11), we have the equivalent resistance

$$R_{\square\times n}(A_{x_1}, P_{x_2}) = \frac{|x_2 - x_1|}{4} r + r_0 \frac{\beta_{1,1}^{(1)} - 2\beta_{1,2}^{(1)} \cos(y\pi/2) + \beta_{2,2}^{(1)}}{4G_n^{(1)}} + r_0 \frac{\beta_{1,1}^{(2)} - 2\beta_{1,2}^{(2)} \cos(y\pi) + \beta_{2,2}^{(2)}}{16G_n^{(2)}}, \quad (111)$$

where P_k represents the nodes of A_k, B_k, C_k, and D_k, and $\beta_{k,s}^{(i)}$ and $G_k^{(i)}$ are, respectively, defined in Eqs. (6) and (7). Equation (111) is a general formula, which can produce several specific results below.

When $x_1 = 0$ and $x_2 = k$, equation (111) reduces to

$$R_{\square\times n}(A_0, P_k) = \frac{k}{4} r + r_0 \frac{h_1 \alpha_{2,n} - 2h_1 \alpha_{2,n-k}^{(1)} \cos(y\pi/2) + \alpha_{1,k}^{(1)} \alpha_{2,n-k}^{(1)}}{4G_n^{(1)}} + r_0 \frac{h_1 \alpha_{2,n}^{(2)} - 2h_1 \alpha_{2,n-k}^{(2)} \cos(y\pi) + \alpha_{1,k}^{(2)} \alpha_{2,n-k}^{(2)}}{16G_n^{(2)}}, \quad (112)$$

where $h_k = r_k/r_0$, $\alpha_{k,s}^{(i)}$ and $G_k^{(i)}$ are, respectively, defined in Eqs. (5) and (7).

When $x_1 = 0$ and $x_2 = n$, equation (112) reduces to

$$R_{\square\times n}(A_0, P_n) = \frac{n}{4} r + r_0 \frac{h_1 \alpha_{2,n} - 2h_1 h_2 \cos(y\pi/2) + h_2 \alpha_{1,n}^{(1)}}{4G_n^{(1)}} + r_0 \frac{h_1 \alpha_{2,n}^{(2)} - 2h_1 h_2 \cos(y\pi) + h_2 \alpha_{1,n}^{(2)}}{16G_n^{(2)}}. \quad (113)$$

When $x_2 = x_1$, equation (111) reduces to

$$R_{\square\times n}(A_{x_1}, P_{x_1}) = r_0 \frac{\beta_{1,1}^{(1)}[1-\cos(y\pi/2)]}{2G_n^{(1)}} + r_0 \frac{\beta_{1,1}^{(2)}[1-\cos(y\pi)]}{8G_n^{(2)}}, \tag{114}$$

where $P_{x_1} = A_{x_1}$ if $y = 0$; $P_{x_1} = B_{x_1}$ if $y = 1$; $P_{x_1} = C_{x_1}$ if $y = 2$; $P_{x_1} = D_{x_1}$ if $y = 3$.

In particular, when $r_1 = r_2 = r_0$, equation (114) reduces to

$$R_{\square\times n}(A_{x_1}, P_{x_1}) = r_0 \frac{\Delta F_{x_1}^{(1)} \Delta F_{n-x_1}^{(1)}[1-\cos(y\pi/2)]}{2F_{n+1}^{(1)}} + r_0 \frac{\Delta F_{x_1}^{(2)} \Delta F_{n-x_1}^{(2)}[1-\cos(y\pi)]}{8F_{n+1}^{(2)}}. \tag{115}$$

Equation (112) is still a complex and general formula, which can still produce several specific results below.

Considering the resistance between two nodes A_0 and A_k, there is $y = 0$, so equation (112) reduces to

$$R_{\square\times n}(A_0, A_k) = \frac{k}{4}r + r_0 \frac{h_1\alpha_{2,n}^{(1)} - 2h_1\alpha_{2,n-k}^{(1)} + \alpha_{1,k}^{(1)}\alpha_{2,n-k}^{(1)}}{4G_n^{(1)}} + r_0 \frac{h_1\alpha_{2,n}^{(2)} - 2h_1\alpha_{2,n-k}^{(2)} + \alpha_{1,k}^{(2)}\alpha_{2,n-k}^{(2)}}{16G_n^{(2)}}. \tag{116}$$

In particular, when $r_1 = r_2 = r_0$ and $k = n$, from Eq. (116) we have

$$R_{\square\times n}(A_0, A_n) = \frac{n}{4}r + r_0 \frac{\Delta F_n^{(1)} - 1}{2F_{n+1}^{(1)}} + r_0 \frac{\Delta F_n^{(2)} - 1}{8F_{n+1}^{(2)}}, \tag{117}$$

where $F_k^{(i)} = (\lambda_i^n - \bar{\lambda}_i^n)/(\lambda_i - \bar{\lambda}_i)$ is defined in Eq. (4).

Considering the resistance between two nodes A_0 and B_k, there is $y = 1$, so equation (112) reduces to

$$R_{\square\times n}(A_0, B_k) = \frac{k}{4}r + r_0 \frac{h_1\alpha_{2,n}^{(1)} + \alpha_{1,k}^{(1)}\alpha_{2,n-k}^{(1)}}{4G_n^{(1)}} + r_0 \frac{h_1\alpha_{2,n}^{(2)} + 2h_1\alpha_{2,n-k}^{(2)} + \alpha_{1,k}^{(2)}\alpha_{2,n-k}^{(2)}}{16G_n^{(2)}}, \tag{118}$$

where $h_k = r_k/r_0$, and $\alpha_{k,s}^{(i)}$ and $G_k^{(i)}$ are, respectively, defined in Eqs. (5) and (7).

In particular, when $r_1 = r_2 = r_0$ and $k = n$, from Eq. (118) we have

$$R_{\square\times n}(A_0, B_n) = \frac{n}{4}r + r_0 \frac{\Delta F_n^{(1)}}{2F_{n+1}^{(1)}} + r_0 \frac{\Delta F_n^{(2)} + 1}{8F_{n+1}^{(2)}}. \tag{119}$$

Considering the resistance between two nodes A_0 and C_k, there is $y = 2$, so equation (112) reduces to

$$R_{\square\times n}(A_0, C_k) = \frac{k}{4}r + r_0 \frac{h_1\alpha_{2,n}^{(1)} + 2h_1\alpha_{2,n-k}^{(1)} + \alpha_{1,k}^{(1)}\alpha_{2,n-k}^{(1)}}{4G_n^{(1)}} + r_0 \frac{h_1\alpha_{2,n}^{(2)} - 2h_1\alpha_{2,n-k}^{(2)} + \alpha_{1,k}^{(2)}\alpha_{2,n-k}^{(2)}}{16G_n^{(2)}}. \tag{120}$$

In particular, when $r_1 = r_2 = r_0$ and $k = n$, from Eq. (120) we have

$$R_{\square\times n}(A_0, C_n) = \frac{n}{4}r + r_0 \frac{\Delta F_n^{(1)} + 1}{2F_{n+1}^{(1)}} + r_0 \frac{\Delta F_n^{(2)} - 1}{8F_{n+1}^{(2)}}. \tag{121}$$

In order to clearly understand the change rule of equivalent resistances $R_{\Delta\times n}(A_0, A_k)$ and $R_{\Delta\times n}(A_0, B_k)$, we use Matlab tool to draw their change curve as shown in Figs. 10 and 11.

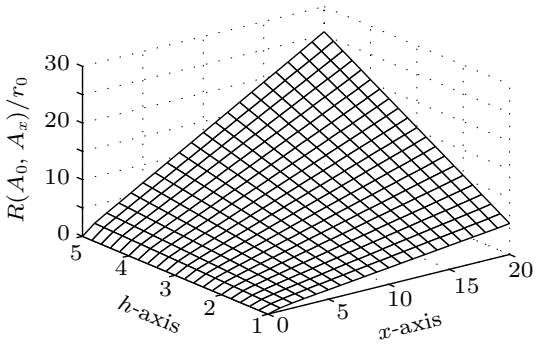

Fig. 10. 3D graph showing equivalent resistance $R(A_0, A_k)$ changing with h and x in $\square \times n$ network, and resistance $R(A_0, A_x)$ increasing with augment of n and x, where $R(A_0, A_0) = 0$ when $x = 0$.

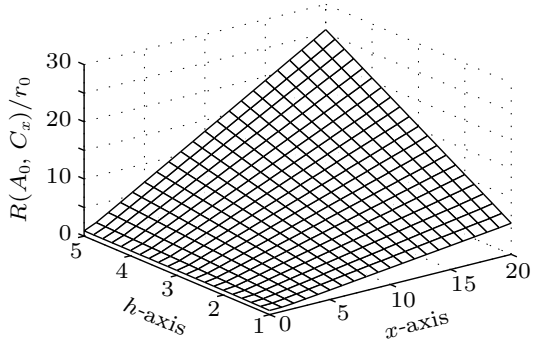

Fig. 11. 3D graph showing equivalent resistance $R(A_0, C_k)$ changing with h and x in $\square \times n$ network, and resistance $R(A_0, C_x)$ incresing with augment of n and x, where $R(A_0, C_0) > 0$ when $x = 0$.

From Figs. 10 and 11, the equivalent resistances $R(A_0,A_k)$ and $R(A_0,C_k)$ increase with t n and x increasing. Comparing Fig. 10 with Fig. 11, we find that their variation patterns are basically similar, but there are slight differences between them, which are $R_{\square\times n}(A_0,A_0)=0$ and $R_{\square\times n}(A_0,C_0)>0$, these are exactly the same as the results of the actual circuit.

In Refs. [33] and [49] the $\square\times n$ circuit network with $r_1=r_2=r_0$ was studied specifically and the results of equivalent resistance between two special nodes, such as the points of A_0,A_n and A_0,C_n and A_0,B_n were obtained (Notice that it is only under the special condition of $r_1=r_2=r_0$). Comparing these results shows that they are exactly the same as the results from Eqs. (115), (117), (119), and (121) in this paper. The comparison among these results verifies their correctness.

The Case H indicates again that general formula (11) is a meaningful and multipurpose result since just a 3D $\square\times n$ resistor network has rich contents and many functions such as Eqs. (111)–(121).

Case I When $m=4$, $n=3$, and $r_1=r_2=0$, figure 1 degrades into an anisotropic crystal as shown in Fig. 12. We will give the equivalent resistance between any two nodes by Eq. (96), which is to further understand the physical meaning of Eq. (96).

We define the coordinates of four nodes: $B_k(1,k)$, $C_k(2,k)$. As $\theta_i=i\pi/2$, $(i=1,2,3)$, then λ_k and $\bar{\lambda}_k$ satisfies Eq. (110), and $\cos(y\theta_1)=\cos(y\theta_3)$. By Eq. (96) we have a general formula

$$R(d_1,d_2)=\frac{|x_2-x_1|}{4}r+\frac{\beta_{1,1}^{(1)}-2\beta_{1,2}^{(1)}\cos(y\pi/2)+\beta_{2,2}^{(1)}}{2F_3^{(1)}}r+\frac{\beta_{1,1}^{(2)}-2\beta_{1,2}^{(2)}\cos(y\pi)+\beta_{2,2}^{(2)}}{4F_3^{(2)}}r, \tag{122}$$

where $\beta_{k,s}^{(i)}=F_{x_k}^{(i)}F_{3-x_s}^{(i)}$. By Eq. (122) we have a special set of results ($h=r/r_0$)

$$R(A_0,A_3)=\frac{3}{4}r, \tag{123}$$

$$R(A_0,B_k)=\frac{1}{4}r+\frac{(h+1)r}{(2h+1)(2h+3)}+\frac{(2h+1)r}{2(4h+1)(4h+3)}, \tag{124}$$

$$R(A_0,C_k)=\frac{1}{2}r+\frac{(h+1)r}{(2h+1)(2h+3)}+\frac{(2h+1)r}{2(4h+1)(4h+3)}, \tag{125}$$

$$R(B_0,B_1)=R(B_0,B_3)=\frac{(h+1)r}{(2h+1)(2h+3)}+\frac{(2h+1)r}{(4h+1)(4h+3)}, \tag{126}$$

$$R(B_0,B_2)=\frac{2(h+1)r}{(2h+1)(2h+3)}, \tag{127}$$

$$R(B_0,C_k)=\frac{1}{4}r+\frac{2(h+1)-\cos(k\pi/2)}{(2h+1)(2h+3)}r+\frac{2(2h+1)-\cos(k\pi)}{2(4h+1)(4h+3)}r, \tag{128}$$

where $k=0$, 1, 2, 3, such as $C_k=\{C_0,C_1,C_2,C_3\}$.

The above results (123)–(128) are a series of equivalent resistances derived from formula (122). The actual calculation is conducted based on Fig. 13, and the obtained results are found to be exactly the same as the above results. This indirectly verifies the correctness of the conclusion (11) given in this paper.

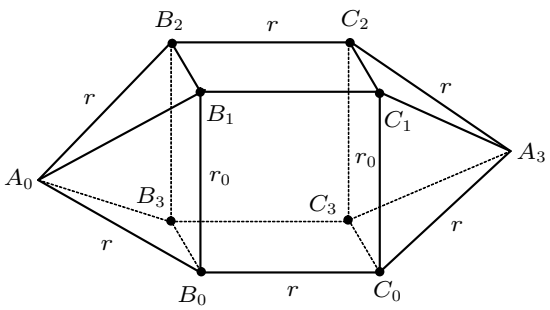

Fig. 12. Crystal lattice with resistors r and r_0 in respective horizontal and vertical directions.

According to the above discussion, the readers should be able to understand the essential meaning of Eq. (11) and understand that equation (11) has broad application value for a variety of lattice structures, which will provide a new theoretical basis for relevant scientific research. As explained in Section 1 and the numerous special cases given above, the theoretical results of this paper will have potential application value in relevant fields.

4.3. Comparison and trigonometric identities

Consider a regular $m\times n$ cylindrical network with $r_1=r_2=r_0$ as shown in Fig. 1. In Ref. [26] there was a resistance formula (1) given by the Laplacian matrix method, which is in the form of double sum. However, in this paper equation (92) is given by the RT-V method, where the condition and network structure are consistent with those in Ref. [26]. Obviously, the two results in the different form, which appear in two

independent articles, are necessarily equivalent because they are from the same network with the same coordinates. Comparing formula (92) with formula (1), and taking y, m, n and x_1, x_2 as natural numbers, when $0 \leqslant x_1 \leqslant x_2 \leqslant n$, $0 \leqslant y \leqslant m-1$, we obtain the following trigonometric identity:

$$\frac{1}{m}\sum_{i=1}^{m-1}\sum_{j=1}^{n}\frac{C_{x_1,j}^2+C_{x_2,j}^2-2C_{x_1,j}C_{x_2,j}\cos(y\theta_i)}{(1-\cos\theta_i)+h^{-1}(1-\cos\phi_j)}=\left(\frac{y^2}{m}-y\right)+\frac{n+1}{2m}\sum_{i=1}^{m-1}\frac{\beta_{1,1}^{(i)}-2\beta_{1,2}^{(i)}\cos(y\theta_i)+\beta_{2,2}^{(i)}}{(1-\cos\theta_i)F_{n+1}^{(i)}}, \tag{129}$$

where $C_{x_k,j}=\cos(x_k+1/2)\phi_j$ with $\phi_j=j\pi/(n+1)$; $\theta_i=2i\pi/m$; $\beta_{k,s}^{(i)}=\Delta F_{x_k}^{(i)}\Delta F_{n-x_s}^{(i)}$; $\Delta F_k^{(i)}=F_{k+1}^{(i)}-F_k^{(i)}$; $F_k^{(i)}=(\lambda_i^k-\bar{\lambda}_i^k)/(\lambda_i-\bar{\lambda}_i)$ with

$$\lambda_i=1+h-h\cos\theta_i+\sqrt{(1+h-h\cos\theta_i)^2-1},\qquad \bar{\lambda}_i=1+h-h\cos\theta_i-\sqrt{(1+h-h\cos\theta_i)^2-1}. \tag{130}$$

In particular, when setting y, m, n and x_1, x_2 to be special number values, we have the following interesting identities.

Deduction 1 When $y=0$, from Eq. (129) we have

$$\frac{2}{n+1}\sum_{i=1}^{m-1}\sum_{j=1}^{n}\frac{[\cos(x_1+1/2)\phi_j-\cos(x_2+1/2)\phi_j]^2}{(1-\cos\theta_i)+h^{-1}(1-\cos\phi_j)}=\sum_{i=1}^{m-1}\frac{\beta_{1,1}^{(i)}-2\beta_{1,2}^{(i)}+\beta_{2,2}^{(i)}}{(1-\cos\theta_i)F_{n+1}^{(i)}}. \tag{131}$$

In particular, when $m=2$, we have $\cos\theta_1=-1$, then equation (131) reduces to

$$\frac{1}{n+1}\sum_{j=1}^{n}\frac{[\cos(x_1+1/2)\phi_j-\cos(x_2+1/2)\phi_j]^2}{2+h^{-1}(1-\cos\phi_j)}=\frac{\beta_{1,1}^{(1)}-2\beta_{1,2}^{(1)}+\beta_{2,2}^{(1)}}{4F_{n+1}^{(1)}}, \tag{132}$$

where $\beta_{k,s}^{(1)}=\Delta F_{x_k}^{(1)}\Delta F_{n-x_s}^{(1)}$, $F_k^{(1)}=(\lambda_1^k-\bar{\lambda}_1^k)/(\lambda_1-\bar{\lambda}_1)$ with

$$\lambda_1=1+2h+2\sqrt{h(1+h)},\qquad \bar{\lambda}_1=1+2h-2\sqrt{h(1+h)}. \tag{133}$$

Deduction 2 When $x_1=x_2=x$, equation (129) reduces to

$$\frac{2}{m}\sum_{i=1}^{m-1}\sum_{j=1}^{n}\frac{\cos^2[(x+1/2)\phi_j](1-\cos y\theta_i)}{(1-\cos\theta_i)+h^{-1}(1-\cos\phi_j)}=\left(\frac{y^2}{m}-y\right)+\frac{n+1}{m}\sum_{i=1}^{m-1}\frac{\Delta F_x^{(i)}\Delta F_{n-x}^{(i)}}{F_{n+1}^{(i)}}\left(\frac{1-\cos(y\theta_i)}{1-\cos\theta_i}\right), \tag{134}$$

where $\phi_j=j\pi/(n+1)$ and $\theta_i=2i\pi/m$.

Deduction 3 When $m=2$, $y=1$, we have $\cos\theta_1=-1$, $\phi_j=j\pi/(n+1)$, from Eq. (129), we have

$$\frac{1}{n+1}\sum_{j=1}^{n}\frac{(C_{x_1,j}+C_{x_2,j})^2}{2+h^{-1}(1-\cos\phi_j)}=\frac{\beta_{1,1}^{(1)}+2\beta_{1,2}^{(1)}+\beta_{2,2}^{(1)}}{4F_{n+1}^{(1)}}-\frac{1}{n+1}, \tag{135}$$

where $C_{x_k,j}=\cos(x_k+1/2)\phi_j$; $F_k^{(1)}=(\lambda_1^k-\bar{\lambda}_1^k)/(\lambda_1-\bar{\lambda}_1)$; λ_1 and $\bar{\lambda}_1$ are given by Eq. (133).

Deduction 4 When $x=n=0$, $\theta_i=2i\pi/m$, $0\leqslant y\leqslant m-1$, and $y\in N$, by Eq. (134) we have

$$\sum_{i=1}^{m-1}\frac{1-\cos(yi\pi/m)}{1-\cos(i\pi/m)}=y(m-y). \tag{136}$$

Note that the identity (129) is found for the first time in this paper. Identity (129) reduces a double sum to a single sum, which provides a new proposition and research method for mathematical researchers.

5. Conclusions and comments

This paper shows a new progress of studying the electrical characteristics (resistance and potential) of an arbitrary cylindrical $m\times n$ resistor network with complex boundaries by the advanced RT-V method, which reveals the electrical characteristics of complex cylindrical network for the first time, such as three general formulae (8), (10), and (11). As the general applications of these three formulas, many interesting results are produced for various types of resistor networks. When the boundary resistor $r_2=0$, the non-regular cylindrical network degrades into a cobweb network as shown in Fig. 3; when the boundary resistor $r_1=r_2=0$, the non-regular cylindrical network degrades into a globe network as shown in Fig. 4; when considering $m=3$ and $m=4$ figure 1 degrades into the $\Delta\times n$ and $\square\times n$ networks. These show that the cylindrical network in Fig. 1 is a kind of complex network with multi-function and multi-structure, which is a network model and scientific problem with great research value. In particular, a new mathematical identity is discovered in the comparative study, which provides a new proposition for mathematical researchers. These

problems discussed above give rise to a series of new results presented in this paper, which fill in the deficiencies of previous literature research,and provide a new theoretical basis for multidisciplinary application. This shows that the RT method has a wide range of applications and can solve a variety of complex resistance network problems, and it has become the basic theory of relevant scientific research in the future.

As is well known, the research of resistor network is mainly a model study, which can explain more problems that have been solved or not solved previously. The present research focuses on how to study and establish the complex network model. Therefore, the discussion emphasizes the research methodology and calculation results of resistor network model. This paper presents the theoretical results of the overall electrical properties of cylindrical networks and discuss a series of special cases for illustrating that the cylindrical network with complex boundary has many special structures, so it has more potential application value. The RT method is mainly used to accurately study the resistor network model with complex boundary conditions, and then the analytical expressions of electrical properties obtained from the network model can be applied to other relevant scientific problems. The limitation of this paper is that it does not give concrete applications in practical problems. However, the relevant problems in the future new technology can be abstracted into the network model at first, and then solved by the theory of electrical properties given in this paper, and the examples can be found from neural networks, artificial intelligence, discrete mathematics, *etc*.

References

[1] Bulgakov E N, Maksimov D N and Sadreev A F 2005 *Phys. Rev. E* **71** 046205
[2] McGurn A R 2000 *Phys. Rev. B* **61** 13235
[3] Albert V V, Glazman L I and Jiang L 2015 *Phys. Rev. Lett.* **114** 173902
[4] Melnikov A V, Shuba M and Lambin P 2018 *Phys. Rev. E* **97** 043307
[5] Barabási A L, Albert R and Jeong H 1999 *Physica A* **272** 173
[6] Cserti J 2000 *Am. J. Phys.* **68** 896
[7] Koutschan C 2013 *J. Phys. A: Math. Theor.* **46** 125005
[8] Joyce G S 2017 *J. Phys. A: Math. Theor.* **50** 425001
[9] Ge D B and Yan Y B 2011 *Finite Difference Time Domain Method of Electromagnetic Wave* (Xi'an: Xidian University Press) p. 10 (in Chinese)
[10] Borges L and Daripa P 2001 *J. Comput. Phys.* **169** 151
[11] Lu J J, Wu X P and Klaus S 2009 *Prog. Geophys.* **24** 154 (in Chinese)
[12] Klein D J and Randić M 1993 *J. Math. Chem.* **12** 81
[13] Chen H Y and Zhang F J 2008 *J. Math. Chem.* **44** 405
[14] Xiao W J and Gutman I 2003 *Theor. Chem. Acc.* **110** 284
[15] Yang Y J and Klein D J 2013 *Disc. Appl. Math.* **161** 2702
[16] Gervacio S V 2016 *Disc. Appl. Math.* **203** 53
[17] Jiang Z Z and Yan W G 2019 *Appl. Math. Comput.* **361** 42
[18] Cao J D, Liu J B and Wang S H 2019 *J. Algebra Appl.* **18** 1950053
[19] Yang Y J and Klein D J 2014 *J. Phys. A: Math. Theor.* **47** 375203
[20] Yang Y J and Zhang H P 2008 *J. Phys. A: Math. Theor.* **41** 445203
[21] Jiang Z Z and Yan W G 2017 *Physica A* **484** 21
[22] Wang Y and Yang X R 2015 *Chin. Phys. B* **24** 118902
[23] Owaidat M Q, Al-Badawi A A, Asad J H and Mohammed AlT 2018 *Chin. Phys. Lett.* **35** 020502
[24] Asad J H 2013 *J. Stat. Phys.* **150** 1177
[25] Owaidat M Q and Asad J H 2016 *Eur. Phys. J. Plus.* **131** 309
[26] Wu F Y 2004 *J. Phys. A: Math. Gen.* **37** 6653
[27] Chair N and Dannoun E M A 2015 *Phys. Scr.* **90** 035206
[28] Izmailian N S, Kenna R and Wu F Y 2014 *J. Phys. A: Math. Theor.* **47** 035003
[29] Essam J W, Izmailian N S, Kenna R and Tan Z Z 2015 *R. Soc. Open Sci.* **2** 140420
[30] Izmailian N S and Kenna R 2014 *J. Stat. Mech.* **9** 1742
[31] Izmailian N S and Kenna R 2014 *Chin. J. Phys.* **53** 040703
[32] Izmailian N S and Kenna R 2014 *Condens. Matter Phys.* **17** 33008
[33] Tan Z Z 2011 *Resistance Network Model* (Xi'an: Xidian University Press) (in Chinese)
[34] Tan Z Z, Essam J W and Wu F Y 2014 *Phys. Rev. E* **90** 012130
[35] Essam J W, Tan Z Z and Wu F Y 2014 *Phys. Rev. E* **90** 032130
[36] Tan Z Z 2015 *Sci. Rep.* **5** 11266
[37] Tan Z Z 2015 *Phys. Rev. E* **91** 052122
[38] Tan Z Z 2015 *Chin. Phys. B* **24** 020503
[39] Tan Z Z 2016 *Chin. Phys. B* **25** 050504
[40] Tan Z Z 2017 *Commun. Theor. Phys.* **67** 280
[41] Tan Zhen, Tan Z Z and Zhou L 2018 *Commun. Theor. Phys.* **69** 610
[42] Tan Zhen and Tan Z Z 2018 *Sci. Rep.* **8** 9937
[43] Tan Z Z 2017 *Chin. Phys. B.* **26** 090503
[44] Tan Zhen, Tan Z Z and Chen J X 2018 *Sci. Rep.* **8** 5798
[45] Zhang J W, Fu N, Yang L, Zhou L and Tan Z Z 2019 *Results Phys.* **15** 102745
[46] Tan Z Z and Tan Zhen 2020 *Phys. Scr.* **95** 035226
[47] Tan Z Z and Tan Zhen 2020 *Acta Phys. Sin.* **69** 020502 (in Chinese)
[48] Tan Z Z and Tan Zhen 2020 *Commun. Theor. Phys.* **72** 055001
[49] Tan Z, Tan Z Z, Asad J H and Owaidat M Q 2019 *Phys. Scr.* **94** 055203